

Editor: #1

We appreciate the editor's insights and helpful comments/suggestions, which helped improve the scientific quality of our manuscript. Basically, we reflected all the comments and suggestions. And, newly added references were in revised manuscript.

1. General comments

Review of the manuscript number AMT-2019-46 submitted to Atmospheric Measurement Techniques and entitled "Validation, comparison, and integration of GOCI, AHI, MODIS, MISR, and VIIRS aerosol optical depth over East Asia during the 2016 KORUS-AQ campaign" by Myungje Choi et al.

The paper describes the aerosol results and analysis from several different polar-orbiting and geostationary satellites. The author give a meaningful topic and we could get a positive comparison response. It will be better that the authors could give more detailed outside validation using several ground-based instruments. Moreover, there should be a detailed description of data filter and validation method. I recommend publication after minor corrections.

2. Major comments

- The authors should have a detailed description for data filter of all the polar-orbiting and geostationary satellites. It will be meaningful if the authors could give the validation results of all the satellite analyzed in the manuscript calculated using a same algorithm.

Ans.) It would be ideal to provide validation results of all satellites using a same algorithm. There have been attempts to develop such a universal algorithm, GRASP, for example. However, algorithms were designed based on satellite instrument characteristics (different number of channels, instrument response functions, orbits, viewing geometries, aerosol models etc.). On top of that, it takes very long time to develop each algorithm. Each aerosol retrieval algorithm has different threshold for pixel masking. Some algorithms which aim to retrieve more AOD pixels despite of increasing error due to signal contamination can set their threshold of pixel masking loosely. In contrast, some other algorithms can focus on the high accuracy as sacrificing pixel numbers. One example of this pixel masking is by clouds. Generally, each aerosol product provides AOD value with subjective quality assurance flag such as “best quality”, or “moderate quality”. Each algorithm has different method and threshold to detect cloud thus it is very difficult to analyze cloud screening impact on the validation. Also, AERONET only provides AOD with cloud-free condition regionally so that comparison between AERONET and satellite AOD already ensures clear condition. The best approach was to select “best quality” AOD pixels based on provided subjective quality flag.

For the validation of L2 product, this study follows the widely-used collocation criteria of Sayer et al. (2014): satellite pixels within a 25 km radius of each AERONET site are spatially averaged, and AERONET data within a ± 30 min window around the satellite measurements are temporally averaged. Note that the 10 min interval AHI AOD data are collocated with

AERONET AOD within a ± 5 min temporal window. Also note that collocated samples are included in the average if at least one measurement is available. These collocation criteria are applied equally to the all the satellite AOD products for the validation.

We tried to unify different spatiotemporal resolution satellite products to common $0.5^\circ \times 0.5^\circ$ daily mean AOD as a concept of Level 3. We evaluated these daily gridded-mean AODs using daily-mean AERONET AOD equally for all products.

- In the manuscript, the authors also used AERONET data to validate the satellite results. It will be better that the authors could use other more ground-based instrument in different stations to validate and have a comparison with the satellites results.

Ans.) SONET data are additionally used for the land AOD validation and below contents are added in the revised manuscript.

(Section 2.9)

SONET measurements during the KORUS-AQ campaign

The Sun-Sky Radiometer Observation Network (SONET) operated by the Institute of Remote Sensing and Digital Earth, Chinese Academy of Sciences also provides aerosol optical and microphysical data from ground-based CIMEL sun-sky radiometer measurement using their own retrieval algorithm (Li et al., 2018). Total 5 SONET sites data (“Harbin”, “Hefei”, “Nanjing”, “Shanghai”, and “Zhoushan”) are used to evaluate satellite land AOD products. The SONET aerosol data and site information during the campaign are available from the AERONET homepage.

(Section 3.3)

Because of limited number of SONET sites, the N is about 5-7 % of AERONET. Statistical metrics using SONET tend to be similar to the comparison with AERONET, but the values of metrics show worse agreement from SONET than AERONET especially in terms of RMSE and f , which is similar to the result of Choi et al. (2018). The AHI ESR, MODIS DT, and VIIRS show consistently positive MB from 0.08 to 0.15. GOCI shows lower R of 0.75, higher RMSE of 0.22, worse f of 0.29, but better MB of -0.03 , compared to the results with AERONET. It can be attributed to high variation of GOCI climatological surface reflectance uncertainty according to sites. MAIAC shows lowest RMSE of 0.15 and MB of 0.03 and highest f of 0.67. MISR also show high f of 0.60 despite a small N of 5. DB shows slightly lower R of 0.82, higher RMSE of 0.21, similar MB of 0.08, and lower f of 0.46 compared to the results using AERONET. The aerosol retrieval algorithm, maintenance, calibration of SONET is different from those of AERONET, thus it is difficult to explain the difference between the two results using AERONET and SONET. Chinese sites seem to have more difficulties to retrieve aerosol properties from most satellite instruments.

Table 1. Validation statistics for land AOD products using SONET.

| Products (resolution) | N | R | RMSE | MB | f within EE _{DT} |
|-----------------------|-----|------|------|---------|-----------------------------|
| GOCI (6 km) | 287 | 0.75 | 0.22 | -0.03 | 0.29 |
| AHI MRM (6 km) | 922 | 0.85 | 0.17 | -0.03 | 0.43 |
| AHI ESR (6 km) | 926 | 0.89 | 0.18 | 0.09 | 0.58 |
| MODIS DT (10 km) | 50 | 0.91 | 0.21 | 0.08 | 0.48 |
| MODIS DT (3 km) | 83 | 0.87 | 0.25 | 0.15 | 0.37 |
| MODIS DB (10 km) | 59 | 0.82 | 0.21 | 0.08 | 0.46 |
| MODIS MAIAC (1 km) | 89 | 0.88 | 0.15 | 0.03 | 0.67 |
| MISR (4.4 km) | 5 | 0.99 | 0.18 | -0.09 | 0.60 |
| VIIRS (0.75 km) | 58 | 0.90 | 0.23 | 0.11 | 0.43 |

- From Figure2, we could find there are difference for the amount of data of different satellite.
The authors should give detailed reasons (Due to errors or cloud?)

Ans.) Discussions are added as below in the Section 4.1.

Additionally, MODIS and VIIRS do not provide spatially continuous AOD distributions because of sun-glint masking over ocean areas near Hokkaido, making identification of plume sources and transport pattern difficult. In contrast, GEO can avoid sun-glint area over mid-latitude area. Sun-glint is a bright ocean surface due to the reflected solar radiance, which is brighter in nadir viewing angle. Due to the measurement geometry, single-angle viewing LEO sensors such as MODIS and VIIRS have the sun-glint pixels in the middle of swath generally. In contrast, GEO has the sun-glint pixels as a circle shape centered at equator because GEO sensors are located at the equator. Because of multi-temporal measurement without sun-glint pixels, GEO such as GOCI and AHI can detect these transported aerosol plumes across ocean with more continuous spatiotemporal distribution than LEO.

- 4, Why the authors only use the GOCI measurements in the case analysis (Section 4.2)

Ans.) Other measurements are also added as in Figures 6 and 7 in the revised manuscript. And, the section 4.2 was revised as below including additional discussions using other satellites.

4.2 Analysis of 25 May 2016 and 5 June 2016 cases over Yellow Sea and Korean Peninsula

Next, two heavy aerosol loading cases over Korean Peninsula are analyzed as in Fig. 6.

During the campaign, the first noticeable increase in PM above the Korean national air-

quality standard ($50 \mu\text{g m}^{-3}$ before April 2018; now $35 \mu\text{g m}^{-3}$) occurred on 25 May 2016
 and resulted in dense aerosol conditions around the Korean Peninsula. In the morning, high
 AOD values ranging from 0.8 to 2.0 were measured by GOCI, AHI, and MISR over the Yellow
 Sea located to the west of the Korean Peninsula. A few land pixels in the southwestern
 Korean Peninsula adjacent to this dense aerosol plume also showed high AOD values of ~ 1.0 .
 Land pixels in the northwestern Korean Peninsula and adjacent ocean pixels were screened
 out because of clouds. Very low AOD values (0.0–0.3) were observed at other land pixels
 over the eastern Korean Peninsula had. Most ocean AOD pixels are screened out from
 MODIS DT and MODIS MAIAC because of sun glint. MISR detect the plume over the Yellow
 Sea, not affected by sun glint with multi-angle imaging capability. As the plume continuously
 moved eastward, high AOD plume entered over land pixels in the Korean Peninsula and a
 steep zonal gradient of AOD was evident near 127°E in the afternoon. To evaluate the
 temporal AOD transportation quantitatively, Hovmöller diagram of GOCI and AHI MRM
 AOD pixels within a box area (123°E – 128°E and 35°N – 38°N) were constructed by averaging
 meridionally at a 0.02° longitude interval as shown in Fig. 7a and b. The peak at 09:30 LST
 was located at $\sim 123.5^\circ\text{E}$ and moved continuously eastward to 123.8°E , 124.4°E , 124.8°E ,
 125.0°E , 125.5°E , 125.8°E , and 126.3°E at 1 h intervals until 16:30 LST. This transport
 corresponds to easterly zonal wind direction at 850 hPa of the Fifth generation of European
 Centre for Medium-Range Weather Forecasts (ECMWF) atmospheric reanalyses of the
 global climate (ERA5; Copernicus Climate Change Service, 2017). The AOD over the Yellow
 Sea (123°E – 126°E) decreased from 1.2 to 0.9 as the plume passed over. In contrast, the AOD
 over the Korean Peninsula (126°E – 129.5°E) increased gradually, particularly over 127°E in
 the western Korean Peninsula where it increased from 0.3 to 0.8. The eastern Korean
 Peninsula (128°E – 129.5°E) was not affected by the plume during daylight hours, and the

AOD remained low (0.2–0.3). More detailed feature can be found from higher temporal resolution of AHI than GOCI. Transport speed of plume center ($AOD > 1.1$) can be estimated about 39 km/h from 123.5°E to 126.0°E during 09:00–15:00 LT.

Compared with conditions on 25 May 2016, the overall AODs on 5 June 2016 over the Yellow Sea and Korean Peninsula was low (0.1–0.2) and the AOD over the Seoul Metropolitan Area (SMA) near 127°E and 37°N was about 0.4–0.6 from GOCI and AHI MRM in the morning as in Fig. 6. The focus here is on SMA AOD, which increased up to 1.0 and dispersed out to surrounding areas in the afternoon. The quantities of MISR AOD in the morning (around 0.4–0.5) and VIIRS AOD in the afternoon (around 1.0) over SMA area is analogous with GOCI, AHI MRM, and MODIS MAIAC. In contrast, changes in AOD was less significant from AHI ESR, MODIS DT, and MODIS DB, because morning AODs were higher (around 1.0) than others (around 0.4–0.5). Because the periphery of the SMA remained under low-AOD conditions and aerosol transport from China through the Yellow Sea was not detected, this increase can be attributed to local emissions. A distinct pattern is evident in the temporal changes of meridional mean AODs shown in Fig. 7b and d. The mean AODs in the region 125.5°E–127.0°E gradually increased from 0.2 to 0.5, whereas the AODs in other areas, including the Yellow Sea and eastern Korean Peninsula, remained constant during daylight hours. Unlike conditions on 25 May, the dense aerosol plume on 5 June grew rapidly over a short period of time from local-area emissions and was transported to the Yellow Sea. The wind was easterly and speed in the afternoon was weaker than the case of 25 May 2016, which resulted in less dispersion pattern of local emission compared to the previous case.

The two events analyzed in this section involved rapid changes in hourly AOD, but have noticeably different spatiotemporal characteristics, leading to high-AOD conditions that are

attributed to either long-range transboundary transport from China or local emissions in Korea (Lee et al., 2019). To accurately assess these types of events, spatiotemporally continuous measurements with minimal data gaps are required, which are currently possible only from GEO measurements.

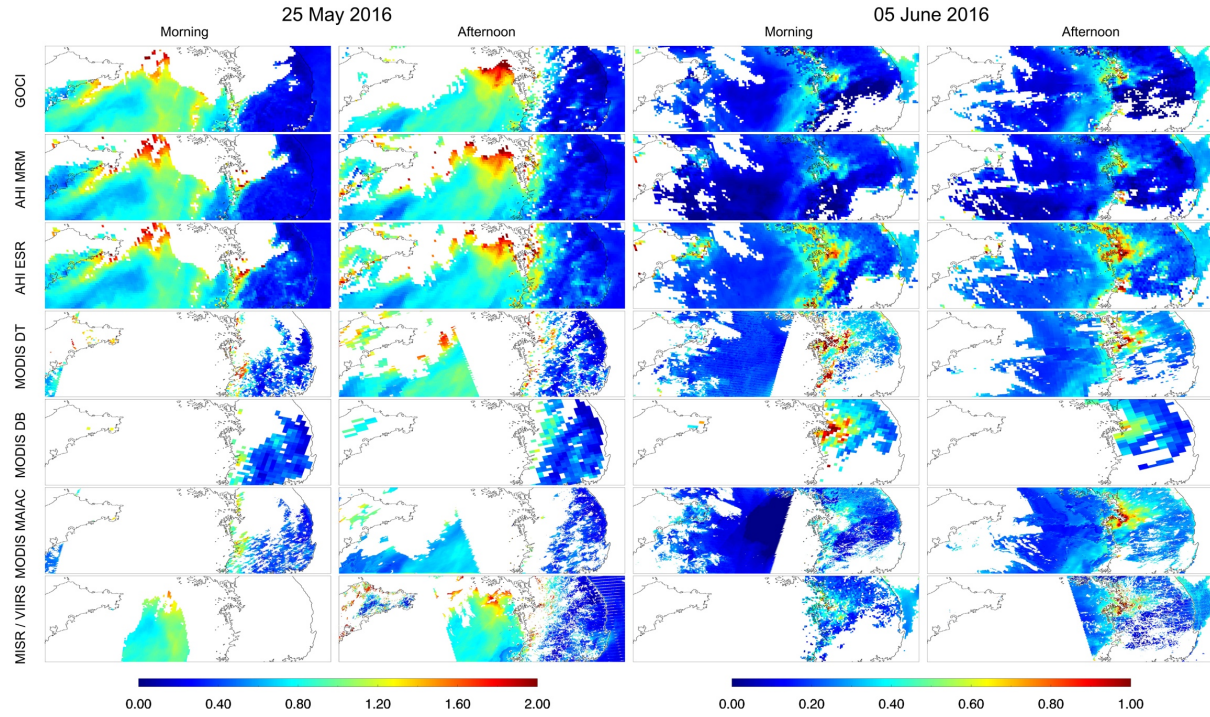


Figure 6. AOD distributions from GOCI, AHI MRM, AHI ESR, MODIS DT03K, MODIS DB, MODIS MAIAC, MISR, and VIIRS over the Yellow Sea and Korean Peninsula (120°E–130°E and 35°N–38°N) at 25 May and 5 June 2016. Local time of morning and afternoon measurements is identical with Fig. 4.

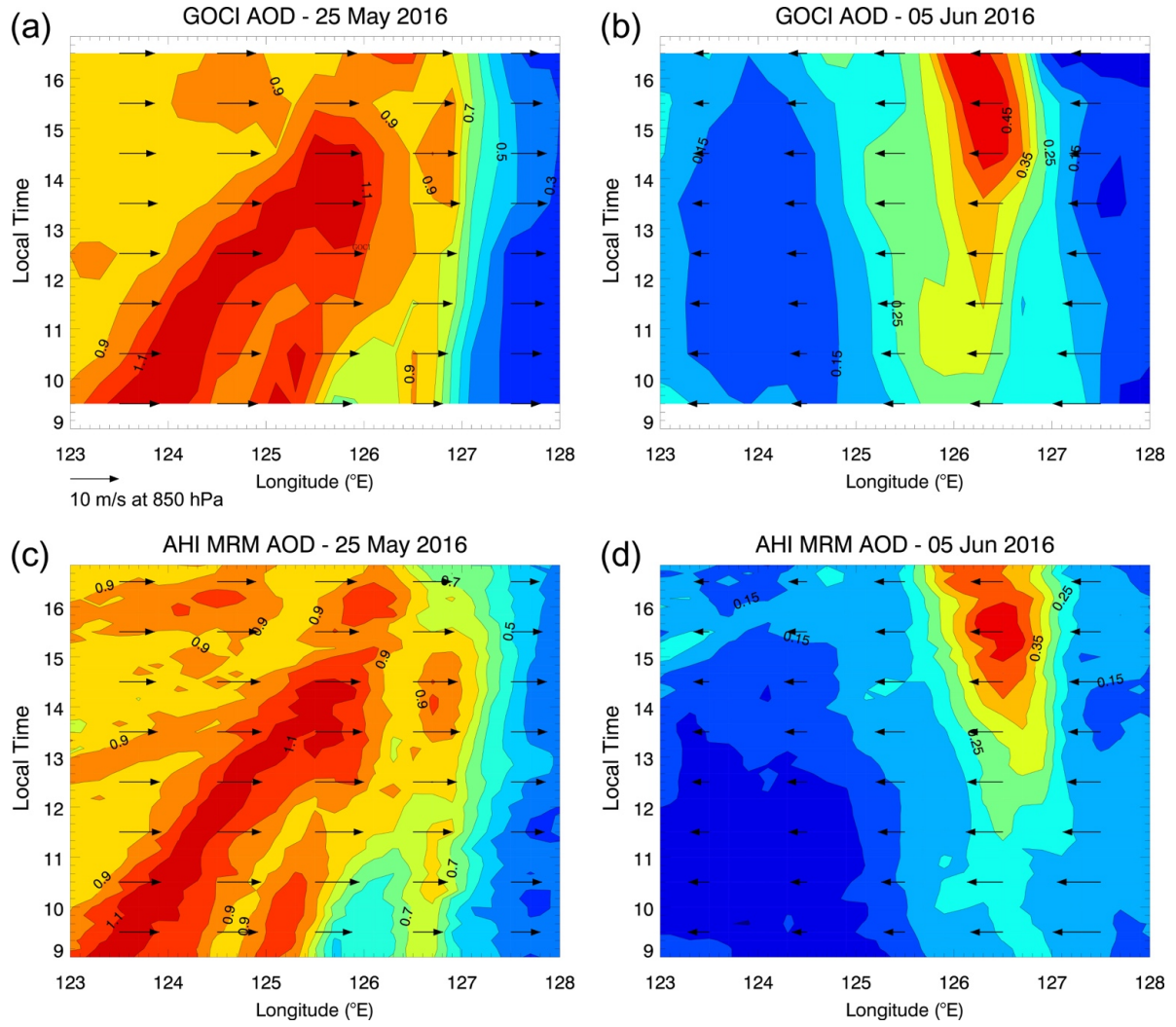


Figure 7. Meridional mean GOCI AOD over the Yellow Sea and the Korean Peninsula (123°E–128°E and 35°N–38°N) at 0.2° longitude intervals on (a) 25 May and (b) 5 June 2016. Meridional mean AHI MRM AOD on (c) 25 May and (d) 5 June 2016. Overlapped arrows represent meridionally averaged zonal wind at 850 hPa.

164 3. Minor comments

165 - Figure2 need to be improved. The font is too small that the readers can't see it clearly.

166 Ans.) The figure was improved as in Fig.4 of the revised manuscript.

167